

## 50 nm Hall Sensors for Room Temperature Scanning Hall Probe Microscopy

Adarsh SANDHU\*, Kouichi KUROSAWA<sup>1</sup>, Munir DEDE<sup>2</sup> and Ahmet ORAL<sup>2</sup>

Research Centre for Quantum Effect Electronics, Tokyo Institute of Technology, 2-12-1 O-okayama, Meguro, Tokyo 152-8552, Japan

<sup>1</sup>Hitachi Science Systems Ltd., 11-1 Ishikawa-Cho, Hitachi City, Ibaraki, 312-0057, Japan

<sup>2</sup>Department of Physics, Bilkent University, Ankara 06533, Turkey

(Received November 5, 2003; accepted November 26, 2003; published February 10, 2004)

Bismuth nano-Hall sensors with dimensions  $\sim 50 \text{ nm} \times 50 \text{ nm}$  were fabricated using a combination of optical lithography and focused ion beam milling. The Hall coefficient, series resistance and optimum magnetic field sensitivity of the sensors were  $4 \times 10^{-4} \Omega/\text{G}$ ,  $9.1 \text{ k}\Omega$  and  $0.8 \text{ G}/\sqrt{\text{Hz}}$ , respectively. A 50 nm nano-Bi Hall sensor was installed into a room temperature scanning Hall probe microscope and successfully used for directly imaging ferromagnetic domains of low coercivity garnet thin films. [DOI: 10.1143/JJAP.43.777]

KEYWORDS: scanning Hall probe microscopy, nanomagnetism, Hall sensors, magnetic domains.

Scanning Hall probe microscopy (SHPM),<sup>1,2)</sup> scanning SQUID,<sup>3)</sup> magnetic force microscopy,<sup>4)</sup> and scanning magnetoresistance microscopy<sup>5)</sup> are examples of the extensive range of scanning probe techniques available for measuring localized magnetic fields at the surfaces of superconducting and ferromagnetic materials.

We have been focusing our attention on the development of high performance room temperature SHPM technology (RT-SHPM) for the non-invasive and direct imaging of localized fluctuations at the surfaces of ferromagnetic materials and recording media using semiconducting GaAs/AlGaAs 2DEG heterostructures and epitaxial InSb micro-Hall probes exhibiting noise levels as low as  $6 \text{ mG}/\sqrt{\text{Hz}}$ .<sup>6–8)</sup> In order to improve the spatial resolution of RT-SHPM it is necessary to overcome drive current limitations due to carrier depletion effects in sub-micron semiconductor devices. As a solution to this problem, we have demonstrated that bismuth (Bi), a semi-metal with a carrier concentration five orders of magnitude lower than metals and negligible surface charge depletion effects,<sup>9)</sup> can be used to fabricate 120 nm sized Hall probes for RT-SHPM.<sup>10)</sup> The micro-Hall probes currently used in our RT-SHPM system incorporate a scanning tunneling tip (STM) for locating the probe into close proximity with the sample surface.<sup>6)</sup> The active ‘cross’ area of the probe is typically 13 micrometers from the STM tip and as shown in Fig. 1, the probe is mounted on a piezoelectric tube (PZT) at a tilt angle of between  $1^\circ$ – $2^\circ$  with respect to the sample surface to ensure that the corner is the closest point to the surface for tunnel current detection and probe positioning during measurements. Further improvements in the spatial resolution requires both a reduction in the physical size of the ‘cross’ area of the Hall probe as well as reducing the probe-to-surface distance by locating the probe much closer to the STM tip whilst maintaining electrical isolation between the probe and STM-tip.

In this short note we describe preliminary results of our study on the fabrication of  $50 \text{ nm} \times 50 \text{ nm}$  Bi nano-Hall probes for RT-SHPM located about 4 micrometers from the STM tip with a noise level of  $0.85 \text{ G}/\sqrt{\text{Hz}}$ ; this noise figure is one order of magnitude better than the  $120 \text{ nm} \times 120 \text{ nm}$  Bi-nano probes, reported previously.

The  $50 \text{ nm} \times 50 \text{ nm}$  Bi nano-Hall probes (nano-BiHP) were fabricated using a combination of conventional

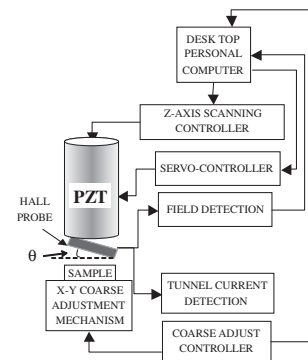


Fig. 1. Main components of the RT-SHPM and probe mounting angle,  $\theta$ .

lithography and focused ion beam (FIB) milling by the following procedure: (i) 60nm thick, polycrystalline Bi thin films were evaporated onto semi-insulating (100) GaAs substrates through patterned photoresist windows from a thermally-heated boat source in a vacuum of  $5 \times 10^{-7}$  Torr, at a rate of 2 nm/s; (ii) a standard lift-off process was used to define ‘Bi squares’  $\sim 15 \mu\text{m} \times 15 \mu\text{m}$  at the corners of the GaAs chips for subsequent FIB milling; (iii)  $400 \mu\text{m} \times 400 \mu\text{m}$  bond pads (30 nm Cr/150 nm Au) were defined by photolithography and lift-off; (iv) photoresist patterning was used to define the STM-tip region, consisting of a window overlapping a  $1 \mu\text{m}$  deep mesa at the chip corner; and finally, (v) STM-tip metals (20 nm Au) were deposited by thermal evaporation followed by liftoff. The resulting Bi micro-Hall probe was then bonded onto packages using  $12 \mu\text{m}$  Au wires.

The nanometer scale dimensions of the active ‘cross’ areas of the resulting Bi micro-Hall probes were defined by FIB ion milling using a Hitachi FB-2100 FIB system. Typical FIB milling conditions employed ion currents and acceleration voltages of  $25 \text{ A}/\text{cm}^2$  and 40 kV, respectively. All FIB milling was carried out at a working distance of 6 mm and with an image resolution of 6 nm. Figs. 2(a) and 2(b) are images of a typical  $50 \text{ nm} \times 50 \text{ nm}$  Bi micro-Hall probe obtained with a Hitachi S-4300 cold field emission scanning electron microscope at an acceleration voltage of 3.0 kV. The nano-BiHP is located approximately 4 micrometers from the STM tip. Particulates on the Hall cross are remnants of the milling process and did not influence the electrical measurements described later.

The optimum drive current of the nano-BiHPs was determined by measuring the noise spectra for a range of

\*E-mail address: sandhu@pe.titech.ac.jp

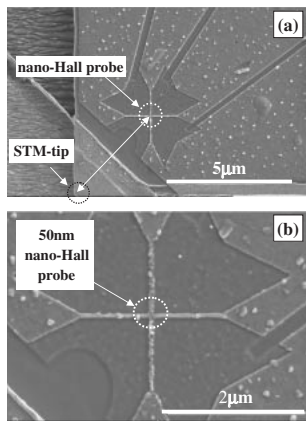


Fig. 2. SEM images of a typical 50 nm Bi nano-Hall probe. (a) Relative locations of the nano-Hall probe and STM-tip. (b) a magnified image of the 50 nm nano-Hall probe of Fig. 4(a).

dc currents using fast Fourier transform signal analyzer. The gain and bandwidth of the Hall amplifier were set to 10,000 and 1 kHz, respectively.

The feasibility of using the nano-Hall sensors for magnetic imaging was tested by mounting the 50 nm  $\times$  50 nm Bi nano-HPs onto the piezoelectric scanning tube of our RT-SHPM at a tilt angle of  $1.2^\circ$  and scanning the devices over a 5  $\mu$ m thick single crystal Bi substituted iron garnet thin film and recording changes in Hall voltage due stray magnetic fields emanating from the surface. Under these measurement conditions, with a tilt angle of  $1.2^\circ$  and STM tip to probe distance of 4  $\mu$ m, the vertical separation between the probe and sample surface was approximately 80 nm, when the STM-tip is in tunneling mode. Thus locating the nano-Hall probe at a distance of 4  $\mu$ m from the STM-tip (compared with 13  $\mu$ m in our previous experiments) devices, drastically improves the spatial resolution using 50 nm nano-HPs.

The room temperature Hall coefficient ( $R_H$ ) and series resistance of the 50 nm  $\times$  50 nm Bi nano-HPs were  $4.0 \times 10^{-4} \Omega/\text{G}$  and 9.1 k $\Omega$ , respectively. The nano HPs were excited with a dc current and the Hall voltage measured using a low noise amplifier located close to the Hall sensor. The minimum detectable magnetic field  $B_{\min}$ , can be defined as  $B_{\min} = V_n/R_H I_{\text{HALL}}$ , where  $V_n$  is the total noise due to the voltage (voltage noise due to the amplifier and noise due to the series resistance of the Hall sensor) at the input of the Hall amplifier.

Figure 3 shows the variation of the minimum detectable field,  $B_{\min}$ , with increasing Hall drive current at a measurement frequency of 1000 Hz. A minimum of  $0.8 \text{ G}/\sqrt{\text{Hz}}$  was

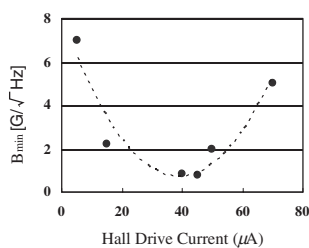


Fig. 3. Variation of the minimum detectable field ( $B_{\min}$ ) with Hall drive current at a measurement frequency of 1000 Hz.

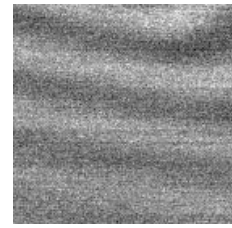


Fig. 4. 8  $\mu\text{m} \times$  8  $\mu\text{m}$  RT-SHPM magnetic image of a 5  $\mu\text{m}$  thick crystalline Bi substituted iron garnet thin film obtained with a drive current of 43  $\mu\text{A}$ .

obtained at a drive current of 43  $\mu\text{A}$ . The increase in noise levels at higher currents is thought to be due to heating effects.

Figure 4 shows a 8  $\mu\text{m} \times$  8  $\mu\text{m}$  RT-SHPM magnetic image of the garnet sample for which we have an extensive set of reference data measured using semiconducting probes and larger Bi micro-Hall probes.<sup>9)</sup> The black and white regions correspond to surface magnetic field changes into and out of the plane of the paper ranging between  $\pm 55\text{G}$ . These values are in excellent agreement with our previous data and these results demonstrate that the Bi-nano Hall probes are functioning properly.

In summary, we described the first ever fabrication of 50 nm  $\times$  50 nm Bi nano-Hall probes with a magnetic field sensitivity of  $0.8 \text{ G}/\sqrt{\text{Hz}}$ , using a combination of conventional photolithography and focused ion beam lithography. The feasibility of using the probes for magnetic imaging was demonstrated by incorporating them into a RT-SHPM system for measurements of stray fields at the surface of magnetic low coercivity garnet thin films. We are currently preparing arrays of thin film ferromagnetic nano-dot structures to quantify the spatial resolution of the 50 nm Bi nano-Hall probes during RT-SHPM measurements. This technology is also expected to find a wide range of applications in areas complementing magnetic force microscopy.

This work was partly funded by the Japanese Ministry of Education, Culture, Sports and Science and Technology (Grant in Aid No. 15560271).

- 1) A. M. Chang, H. D. Hallen, L. Harriott, H. F. Hess, H. L. Kao, J. Kwo, R. E. Miller, R. Wolfe, J. Van Der Ziel and T. Y. Chang: Appl. Phys. Lett. **61** (1992) 1974.
- 2) Oral, S. J. Bending and M. Henini: Appl. Phys. Lett. **69** (1996) 1324.
- 3) K. A. Moler, J. R. Kirtley, R. Liang, D. Bonn and W. N. Hardy: Phys. Rev. B **55** (1997) 12753.
- 4) Y. Martin, D. Rutger and H. K. Wickramasinghe: Appl. Phys. Lett. **52** (1988) 244.
- 5) M. Nakamura, M. Kimura, K. Sueoka and K. Mukasa: Appl. Phys. Lett. **80** (2002) 2713.
- 6) A. Sandhu, H. Masuda, A. Oral, S. J. Bending: Jpn. J. Appl. Phys. **40** (2001) 4321.
- 7) A. Sandhu, N. Iida, H. Masuda, A. Oral, S. J. Bending: J. Magn. Magn. Mater **242-245** (2002) 1249.
- 8) A. Oral, M. Kaval, M. Dede, H. Masuda, A. Okamoto, I. Shibusaki and A. Sandhu: IEEE Trans. Magn. **38** (2002) 2438.
- 9) A. Sandhu, A. Oral, H. Masuda and S. J. Bending: Jpn. J. Appl. Phys. **40** (2001) L524.
- 10) A. Sandhu, H. Masuda, A. Oral, K. Kurosawa and S. J. Bending: Elect. Lett. **37** (2001) 1335.